

The isentropic equation of state of (2+1)-flavor QCD: An update based on high precision Taylor expansion and Padé-resummed expansion at finite chemical potentials

Jishnu Goswami^{a,*} (HotQCD collaboration)

^a*RIKEN Center for Computational Science,
Kobe 650-0047, Japan*

E-mail: jishnu.goswami@riken.jp

The HotQCD Collaboration performed Taylor expansion calculations in 2017 for the pressure, energy density, and entropy density at non-zero chemical potentials up to the 6th order. Since then, they have significantly improved the statistics for lattices with temporal extents of $N_\tau = 8$ and 12, and have also included results for $N_\tau = 16$ that were not previously available. They have also calculated the 8th-order expansion coefficients for $N_\tau = 8$. These calculations showed that the Taylor series expansion for the pressure is accurate up to $\mu_B/T \leq 2.5$. In this study, we use the high-statistics results on Taylor expansion coefficients, calculated with HISQ fermions and extrapolated to the continuum limit, to determine the QCD equation of state under conditions relevant for hot and dense matter produced in heavy ion collisions. We also calculate the energy density and pressure along lines of constant entropy per net baryon number.

The 39th International Symposium on Lattice Field Theory, LATTICE2022 26th-30th July, 2022 Bonn, Germany

*Speaker

1. Introduction

Quantum chromodynamics (QCD) is studied at finite temperature and chemical potential in order to understand the properties of hot and dense matter created in heavy ion collision (HIC) experiments. To describe the state of the matter at extreme conditions, the equation of state (EoS) of QCD in the grand canonical ensemble at finite temperature and non-zero chemical potentials is important. This EoS is an essential input for interpreting heavy ion data [1] in thermal equilibrium and for hydrodynamic modeling of matter created in HIC experiments. It is also used in the analysis of the ‘‘cosmic trajectory’’ [2] at high temperature and low chemical potentials, and for the EoS of neutron star mergers [3, 4] at low temperature and high chemical potentials.

The EoS of (2+1)-flavor QCD, or the relationship between the pressure, energy density, entropy density and temperature of a system, has been well studied at vanishing chemical potential using lattice techniques in [5–7]. However, it is difficult to calculate the EoS at non-vanishing chemical potentials due to the sign problem. Currently, the most commonly used methods for determining the EoS at non-vanishing chemical potentials are Taylor expansion and analytic continuation, both of which have their own strengths and limitations. Taylor expansion, analytic continuation and various resummation technique have been used recently to analyze the EoS at non-vanishing values of the chemical potentials for baryon number, electric charge, and strangeness in previous lattice QCD calculations [8–14].

Recently, we proposed the use of the Padé approximation [15] to improve upon ordinary Taylor expansions of pressure, which we hope will also increase the reliability of the EoS at finite chemical potentials. We have updated our previous analysis of the EoS of (2+1)-flavor QCD using a large data set of gauge field configurations generated using SIMULATEQCD [16] with the HISQ action. A new data set for $N_\tau = 16$ and a larger data set for temperatures between 125-175 MeV were used to update our analysis of the EoS in (2+1)-flavor QCD using the HISQ/tree action. The increased statistics, which include approximately 1.5 million configurations on $32^3 \times 8$ lattices at the pseudo-critical temperature of 156.5(1.5) MeV, allowed us to extend our previous Taylor series results to eighth-order in the chemical potentials. We use the publicly available AnalysisToolbox [17] for most of the data analysis in this proceeding.

2. Taylor expansion and Padé resummation of bulk thermodynamics

The notation used for the Taylor expansions of bulk thermodynamic observables in (2+1)-flavor QCD is outlined in [18]. For ease of reference, we provide a brief summary below,

$$\frac{P}{T^4} = \hat{p} = \frac{1}{VT^3} \ln Z(T, V, \vec{\mu}) = \sum_{i,j,k=0}^{\infty} \frac{\chi_{ijk}^{BQS}}{i!j!k!} \hat{\mu}_B^i \hat{\mu}_Q^j \hat{\mu}_S^k, \quad (1)$$

$$\hat{\epsilon} = \frac{1}{VT^3} T \frac{\partial \ln Z(T, V, \hat{\mu}_B, \hat{\mu}_Q, \hat{\mu}_S)}{\partial T} = \sum_{i,j,k=0}^{\infty} \frac{\Xi_{ijk}^{BQS} + 3\chi_{ijk}^{BQS}}{i!j!k!} \hat{\mu}_B^i \hat{\mu}_Q^j \hat{\mu}_S^k, \quad (2)$$

$$\hat{s} = \hat{\epsilon} + \hat{p} - \hat{\mu}_B \hat{n}_B - \hat{\mu}_Q \hat{n}_Q - \hat{\mu}_S \hat{n}_S. \quad (3)$$

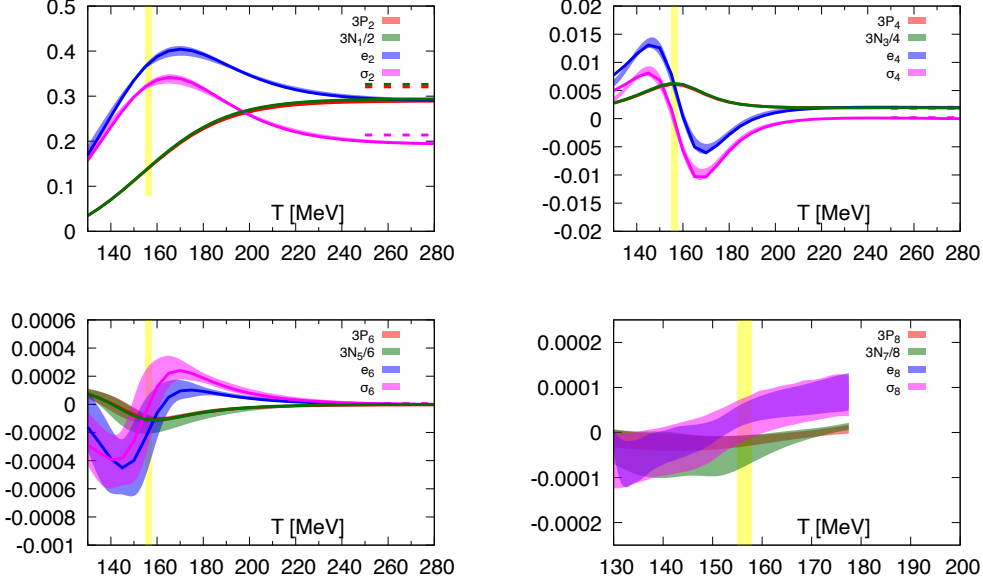


Figure 1: Second-order (top, left), fourth-order (top, right), sixth-order (bottom, left) and eighth-order (bottom, right) expansion coefficients of pressure (P_{2k}), net baryon number density (N_{2k-1}), energy density (ϵ_{2k}) and entropy density (σ_{2k}) for a strangeness-neutral medium ($n_S = 0$) with electric charge to baryon-number density $n_Q/n_B = r = 0.4$. The solid lines are constructed from the parametrization in Table 1.

with $\hat{\mu}_X \equiv \mu_X/T$. χ_{ijk}^{BQS} and Ξ_{ijk}^{BQS} can be written as,

$$\chi_{ijk}^{BQS} = \left. \frac{1}{VT^3} \frac{\partial \ln Z(T, V, \vec{\mu})}{\partial \hat{\mu}_B^i \partial \hat{\mu}_Q^j \partial \hat{\mu}_S^k} \right|_{\vec{\mu}=0}, \quad \Xi_{ijk}^{BQS} = \frac{T d\chi_{ijk}^{BQS}}{dT}, \quad i + j + k \text{ even}. \quad (4)$$

We will study matter that is strangeness neutral ($n_S = 0$) at a fixed ratio of electric charge to baryon number ($n_Q/n_B = r$) by introducing constraints on the electric charge and strangeness chemical potentials. This makes $\hat{\mu}_Q$ and $\hat{\mu}_S$ functions of T and $\hat{\mu}_B$, and hence we can expand

$$\begin{aligned} \hat{\mu}_S(T, \hat{\mu}_B) &= s_1(T)\hat{\mu}_B + s_3(T)\hat{\mu}_B^3 + s_5(T)\hat{\mu}_B^5 + s_7(T)\hat{\mu}_B^7 \\ \hat{\mu}_Q(T, \hat{\mu}_B) &= q_1(T)\hat{\mu}_B + q_3(T)\hat{\mu}_B^3 + q_5(T)\hat{\mu}_B^5 + q_7(T)\hat{\mu}_B^7. \end{aligned} \quad (5)$$

The explicit expressions of q_i and s_i for $i = 1, 3, 5, 7$ can be found in [19, 20]. By substituting the expressions of μ_Q and μ_S using Eq. 5, one can calculate the Taylor series expansion for the number density, the $\hat{\mu}_B$ -dependent part of the pressure, the energy density, and the entropy density,

$$\frac{n_B}{T^3} = \sum_{k=1}^{\infty} N_{2k-1}(T) \hat{\mu}_B^{2k-1} \quad (6)$$

$$\frac{\Delta O}{T^4} = \frac{O(T, \mu_B) - O(T, 0)}{T^4} = \sum_{k=1}^{\infty} O_{2k}(T) \hat{\mu}_B^{2k}, \quad \text{where } O = P, \epsilon, \quad (7)$$

$$\frac{\Delta s}{T^3} = \frac{s(T, \mu_B) - s(T, 0)}{T^3} = \sum_{k=1}^{\infty} \sigma_{2k}(T) \hat{\mu}_B^{2k}. \quad (8)$$

The expansion coefficient of the number density and electric charge chemical potentials will be related to other observables in the following way,

$$P_{2n} = \frac{1}{2n} \left(N_{2n-1}^B + r \sum_{k=1}^n (2k-1) q_{2k-1} N_{2n-2k+1}^B \right) \quad (9)$$

$$P'_{2n} = \frac{1}{2n} \left(N_{2n-1}^{B'} + r \sum_{k=1}^n (2k-1) (q'_{2k-1} N_{2n-2k+1}^B + q_{2k-1} N_{2n-2k+1}^{B'}) \right) \quad (10)$$

$$\epsilon_{2n} = 3P_{2n} + TP'_{2n} - r \sum_{k=1}^n T q'_{2k-1} N_{2n-2k+1}^B \quad (11)$$

$$\sigma_{2n} = 4P_{2n} + TP'_{2n} - N_{2n-1}^B - r \sum_{k=1}^n (q_{2k-1} + T q'_{2k-1}) N_{2n-2k+1}^B. \quad (12)$$

In Fig. 1, we present the results for the expansion coefficients of the pressure series, as well as those for the number density, energy density and entropy density for $r = 0.4$. For $n = 1$ and 2, the coefficients for the energy density and entropy density have been extrapolated to the continuum limit. For $n = 3$ and 4, we provide spline interpolations of the results obtained using $N_\tau = 8$.

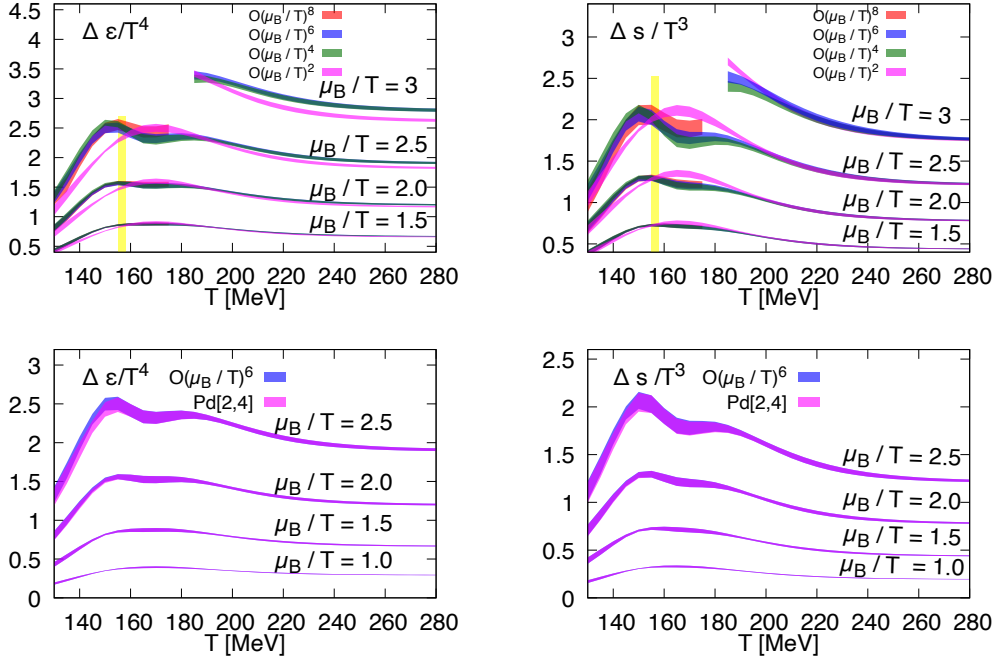


Figure 2: Comparison of different (top) order Taylor expansion results for $\Delta\epsilon/T^4$ with corresponding [2,4] Padé approximants. The yellow bands highlight the $T_{pc} = 156.5(1.5)$ MeV.

In order to understand the range of validity of energy density and entropy density as a function of baryon chemical potential, we will use Taylor series and Padé approximants to compare different orders. Our focus will be on strangeness-neutral matter with a ratio of electric charge density to baryon number density of $r = 0.4$, which is seen in heavy ion collision experiments where the net strangeness number density is zero and the ratio of net electric charge to net baryon number

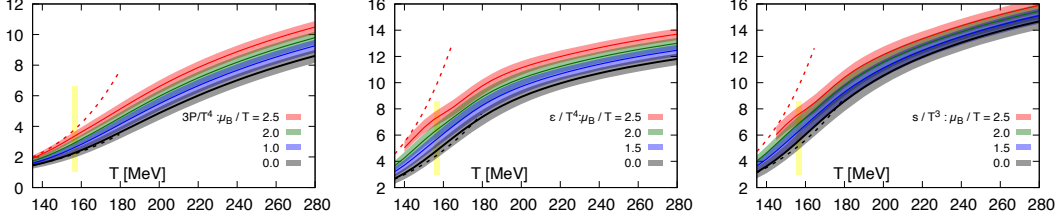


Figure 3: Pressure (left), energy (middle) and entropy (right) densities versus temperature for several values of the baryon chemical potential. Figures show results for the case $n_S = 0$, $n_Q/n_B = 0.4$ in the temperature interval [130 MeV:280 MeV]. The results and parametrization for $\hat{\mu}_B = 0$ were taken from [6]. The solid lines are produced using the parametrization listed in Table 1, while the dotted lines are based on the QMHRG2020 [22, 23] calculation.

density is 0.4 [18]. As part of our analysis, we will define the [2,4] Padé approximant for energy and entropy densities,

$$\left(\frac{\Delta\epsilon(T, \mu_B)}{T^4} \right)_{[2,4]} = \frac{\epsilon_2^2}{\epsilon_4} \frac{\bar{x}^2}{1 - \bar{x}^2 + (1 - c_{6,2})\bar{x}^4}, \bar{x} = \sqrt{\epsilon_4/\epsilon_2} \hat{\mu}_B, c_{6,2} = \frac{\epsilon_6\epsilon_2}{\epsilon_4^2}. \quad (13)$$

$$\left(\frac{\Delta s(T, \mu_B)}{T^3} \right)_{[2,4]} = \frac{\sigma_2^2}{\sigma_4} \frac{\bar{x}^2}{1 - \bar{x}^2 + (1 - c_{6,2})\bar{x}^4}, \bar{x} = \sqrt{\sigma_4/\sigma_2} \hat{\mu}_B, c_{6,2} = \frac{\sigma_6\sigma_2}{\sigma_4^2}. \quad (14)$$

In Fig. 2, we present the energy density (top, left) and entropy density (top, right) for various values of $\hat{\mu}_B$ as a function of temperature. We have found that for high temperatures ($T \gtrsim 200$ MeV), the Taylor series quickly converges for these observables, as reported in [21]. We also show results for larger chemical potentials, such as $\hat{\mu}_B \simeq 3$, for energy and entropy density at temperatures above 200 MeV. In Fig. 2 (bottom, left), we compare the results of the 6th-order Taylor series for $\Delta\epsilon$ with the corresponding [2,4] Padé approximants introduced in Eq.13. We see that the Taylor series and the [2,4] Padé approximants agree well up to a baryon chemical potential of $\mu_B/T \gtrsim 2.5$. However, at the highest chemical potential, the energy density becomes somewhat “wiggly.” The reliability of the energy density is therefore limited to $2 < \mu_B/T < 2.5$. Similar conclusions can be drawn from the comparison of the Taylor expansion and Padé approximant of the entropy density show in Fig. 2 (bottom, right).

3. Parametrization of the EoS of (2+1)-flavor QCD

In Fig. 3, we present the total pressure (left), energy (middle), and entropy (right) densities for $\hat{\mu}_B \in [0 : 2.0]$ at all temperatures analyzed. For $\hat{\mu}_B = 2.5$, we only show results for energy and entropy density at temperatures $T \geq 140$ MeV. The EoS at fixed $\{n_S = 0, n_Q/n_B = 0.4, \mu_B/T\}$ is represented by these results. In this section, we will also update the parametrization for $\mu_B > 0$ from [18]. The N_k 's and q_k 's (where $k = 1, 3, 5$) can be used to create all expansion coefficients of the bulk thermodynamic observables, as shown by Eq. (9-12). The functional forms of the N_k 's and q_k 's are defined as follows:

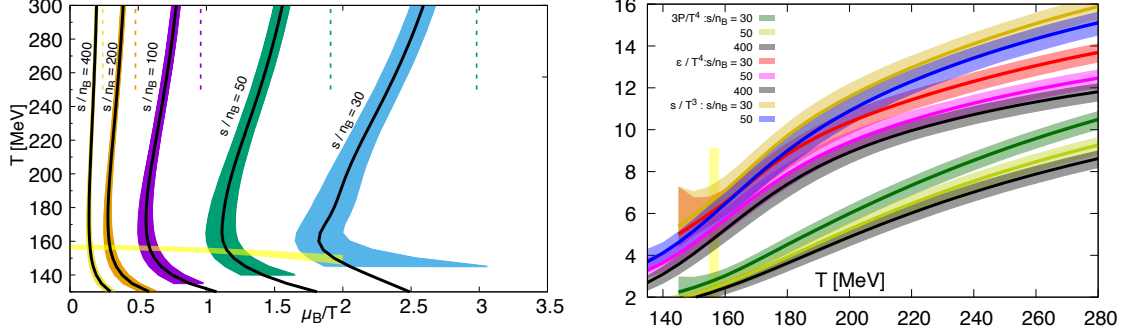


Figure 4: Lines of constant entropy per baryon number (left) in the $T-\hat{\mu}_B$ plane. Pressure, energy and entropy densities (right) versus temperature in constant s/n_B trajectories.

k	$N_{k,0n}^B$	$N_{k,1n}^B$	$N_{k,2n}^B$	$N_{k,3n}^B$	$N_{k,4n}^B$	$N_{k,1d}^B$	$N_{k,2d}^B$	$N_{k,3d}^B$	$N_{k,4d}^B$
1	0.181146	-0.42891324	0.40657622	-0.14809017	0.00584306	-2.79490041	3.91094903	-3.26388671	1.33731772
3	-0.00553136	0.04533642	-0.09913670	0.08379059	-0.02394836	-0.17023948	-1.82763726	0.0	1.05942220
5	1.3211e-04	-9.0274e-04	0.00227410	-0.00247477	9.5899e-04	-1.06474394	0.19724813	-1.02866873	0.95555405
k	$q_{k,0n}$	$q_{k,1n}$	$q_{k,2n}$	$q_{k,3n}$	$q_{k,4n}$	$q_{k,1d}$	$q_{k,2d}$	$q_{k,3d}$	$q_{k,4d}$
1	-0.04047945	0.11134466	-0.12450449	0.06478750	-0.01337327	-2.93860831	3.79902478	-2.61981879	0.84469060
3	3.4415e-04	-0.00112178	0.00120661	-3.5765e-04	-8.2661e-05	-3.73942745	5.37449512	-3.55442936	0.92870411
5	-3.8228e-05	1.5320e-04	-2.5454e-04	2.0114e-04	-6.0832e-05	-2.29784880	1.47464250	0.0	-0.17185948

Table 1: The parameter values can be utilized to build the $\hat{\mu}_B$ dependent part of the equation of state.

$$N_k^B = \frac{N_{k,0n}^B + N_{k,1n}^B \bar{t} + N_{k,2n}^B \bar{t}^2 + N_{k,3n}^B \bar{t}^3 + N_{k,4n}^B \bar{t}^4}{1 + N_{k,1d}^B \bar{t} + N_{k,2d}^B \bar{t}^2 + N_{k,3d}^B \bar{t}^3 + N_{k,4d}^B \bar{t}^4}, \quad k = 1, 3, 5. \quad (15)$$

$$q_k = \frac{q_{k,0n} + q_{k,1n} \bar{t} + q_{k,2n} \bar{t}^2 + q_{k,3n} \bar{t}^3 + q_{k,4n} \bar{t}^4}{1 + q_{k,1d} \bar{t} + q_{k,2d} \bar{t}^2 + q_{k,3d} \bar{t}^3 + q_{k,4d} \bar{t}^4}, \quad k = 1, 3, 5. \quad (16)$$

Here $\bar{t} = T_0/T$ with an arbitrary temperature scale $T_0 = 154$ MeV used as a normalization. The values of the parameters used in these functions are listed in Table 1. The temperature derivatives can be obtained by taking the analytical derivatives of these functions. The consistency of this parametrization is tested on the expansion coefficients shown in Fig. 1. By combining the parametrization found in Table 1 with the $\mu_B = 0$ parametrization found in [6], we have produced the central lines shown in Fig. 3. The provided parametrization for p, ϵ, s at non-zero chemical potential accurately describes the lattice QCD data in the temperature range $T \in [135 : 280]$ and chemical potential $\mu_B/T \in [0 : 2.5]$. These parametrization can also be used to calculate speed of sound and other transport coefficients.

In heavy ion experiments, strongly interacting matter is created when nuclei collide and then its expand and cool while following lines of constant entropy per net baryon number. Thus, to obtain an EoS for fixed $\{n_S = 0, n_Q/n_B = 0.4, s/n_B\}$ we must solve Eq. 17 for μ_B/T to determine

s/n_B	T_{pc} [MeV]	μ_B/T	p [MeV/fm ³]	ϵ [MeV/fm ³]	s [MeV/fm ²]
400	155	0.15(2)	55(7)	355(42)	512(60)
50	150	1.2(1)	47(6)	301(35)	446(52)
30	145	2.5(6)	48(9)	336(83)	525(107)

Table 2: Value of pressure, energy and entropy density for different s/n_B and corresponding T and μ_B/T .

the μ_B/T vs. T trajectories that keep s/n_B fixed [24].

$$\frac{s}{n_B} = \frac{\sigma_0 + \sum_{k=1}^{\infty} \sigma_{2k}(T) \hat{\mu}_B^{2k}}{\sum_{k=1}^{\infty} N_{2k-1}(T) \hat{\mu}_B^{2k-1}} \quad (17)$$

In Figure 4 (left), we plot the μ_B/T against temperature (T) for various values of s/n_B . It can be observed that μ_B/T remains relatively constant at temperatures above 250 MeV for fixed s/n_B values greater than 100. However, for smaller s/n_B values, μ_B/T increases at both high and low temperatures. We also compare these curves to those of ideal gas curves and find that the deviation is approximately 20% for all s/n_B values at the highest temperature. Additionally, we used the previously mentioned parametrization to calculate these trajectories and plotted them as black solid lines.

In Fig. 4 (right), we present the temperature dependence of pressure, energy, and entropy densities at fixed s/n_B trajectories. These observables exhibit similar behavior to those obtained at fixed $\hat{\mu}_B$, as shown in Fig. 3. However, above the pseudo-critical temperature, we observe a sharp increase in these observables for smaller s/n_B as the μ_B/T increases at high temperatures. We also include solid lines representing the parametrization of p , ϵ , and s on fixed s/n_B trajectories in these figures. In Table 2, we provide some preliminary numbers for the pressure, energy and entropy density near the pseudo-critical temperature $T_{pc}(T, \mu_B/T) = T_{pc,0}(1 - \kappa_2(\mu_B/T)^2)$ [25]. The EoS for fixed s/n_B calculated here is applicable to the range of beam energies currently accessible by BES-II at RHIC in collider mode, which is $7.7 \text{ GeV} \leq \sqrt{s_{NN}} \leq 200 \text{ GeV}$.

4. Summary

In this study, we focused on the Taylor expansion of various thermodynamic quantities, such as pressure, energy, and entropy densities, for strange neutral matter with a electric charge to baryon number density ratio of $r = 0.4$. We observed that $\hat{\mu}_B$ dependent part of these observables converge faster to their ideal gas values at high temperatures. We also developed the equation of state for this matter and found that it can be accurately described using Padé approximants. Our comparison of Taylor expansions and Padé approximants at certain $\hat{\mu}_B$ values has given us confidence in the validity of our Taylor expansion results within a range that varies from $\hat{\mu}_B \simeq 2.5$ at low temperatures to $\hat{\mu}_B \gtrsim 3$ at temperatures above 200 MeV. Additionally, we have updated the parametrization of the EoS for the μ_B -dependent part. We also present the EoS of (2+1)-flavor QCD on the fixed s/n_B trajectories relevant for BES II at RHIC.

In the future, we aim to smooth out the "wiggles" observed in energy and entropy densities at $\mu_B/T = 2.5$ by constructing Padé approximants for these quantities using the pressure Padé and utilizing thermodynamic relations. This method has been successfully applied for the vanishing electric charge chemical potential in [21].

Acknowledgements

This work was supported by the DFG Collaborative Research Centre 315477589-TRR 211, "Strong interaction matter under extreme conditions". We thank all the members of the HotQCD collaboration for very helpful discussions.

References

- [1] P. Braun-Munzinger, V. Koch, T. Schäfer and J. Stachel, *Properties of hot and dense matter from relativistic heavy ion collisions*, *Phys. Rept.* **621** (2016) 76 [1510.00442].
- [2] M. M. Middeldorf-Wygas, I. M. Oldengott, D. Bödeker and D. J. Schwarz, *Cosmic QCD transition for large lepton flavor asymmetries*, *Phys. Rev. D* **105** (2022) 123533 [2009.00036].
- [3] C. Drischler, S. Han, J. M. Lattimer, M. Prakash, S. Reddy and T. Zhao, *Limiting masses and radii of neutron stars and their implications*, *Phys. Rev. C* **103** (2021) 045808 [2009.06441].
- [4] Y. Fujimoto, K. Fukushima, L. D. McLerran and M. Praszalowicz, *Trace anomaly as signature of conformality in neutron stars*, 2207.06753.
- [5] F. Karsch, E. Laermann and A. Peikert, *The Pressure in two flavor, (2+1)-flavor and three flavor QCD*, *Phys. Lett. B* **478** (2000) 447 [hep-lat/0002003].
- [6] A. Bazavov et al., *Equation of state in (2+1)-flavor QCD*, *Phys. Rev. D* **90** (2014) 094503 [1407.6387].
- [7] S. Borsanyi, Z. Fodor, C. Hoelbling, S. D. Katz, S. Krieg and K. K. Szabo, *Full result for the QCD equation of state with 2+1 flavors*, *Phys. Lett. B* **730** (2014) 99 [1309.5258].
- [8] R. V. Gavai and S. Gupta, *The Critical end point of QCD*, *Phys. Rev. D* **71** (2005) 114014 [hep-lat/0412035].
- [9] S. Mitra, P. Hegde and C. Schmidt, *New way to resum the lattice QCD Taylor series equation of state at finite chemical potential*, *Phys. Rev. D* **106** (2022) 034504 [2205.08517].
- [10] S. Mitra and P. Hegde, *New formalism for unbiased exponential resummation of Lattice QCD Taylor series at finite baryon chemical potential*, 2209.11937.
- [11] S. Borsanyi, J. N. Guenther, R. Kara, Z. Fodor, P. Parotto, A. Pasztor et al., *Resummed lattice QCD equation of state at finite baryon density: Strangeness neutrality and beyond*, *Phys. Rev. D* **105** (2022) 114504 [2202.05574].

- [12] C. Schmidt, J. Goswami, G. Nicotra, F. Ziesché, P. Dimopoulos, F. Di Renzo et al., *Net-baryon number fluctuations*, [2101.02254](#).
- [13] G. Nicotra, P. Dimopoulos, L. Dini, F. Di Renzo, J. Goswami, C. Schmidt et al., *Lee-Yang edge singularities in 2+1 flavor QCD with imaginary chemical potential*, *PoS LATTICE2021* (2022) 260 [[2111.05630](#)].
- [14] P. Dimopoulos, L. Dini, F. Di Renzo, J. Goswami, G. Nicotra, C. Schmidt et al., *Contribution to understanding the phase structure of strong interaction matter: Lee-Yang edge singularities from lattice QCD*, *Phys. Rev. D* **105** (2022) 034513 [[2110.15933](#)].
- [15] D. Bollweg, J. Goswami, O. Kaczmarek, F. Karsch, S. Mukherjee, P. Petreczky et al., *Taylor expansions and Padé approximants for cumulants of conserved charge fluctuations at nonvanishing chemical potentials*, *Phys. Rev. D* **105** (2022) 074511 [[2202.09184](#)].
- [16] D. Bollweg, L. Alenkort, D. A. Clarke, O. Kaczmarek, L. Mazur, C. Schmidt et al., *HotQCD on multi-GPU Systems*, *PoS LATTICE2021* (2022) 196 [[2111.10354](#)].
- [17] “AnalysisToolbox: A set of Python tools for analyzing physics data, in particular targeting lattice QCD.” <https://github.com/LatticeQCD/AnalysisToolbox>.
- [18] A. Bazavov et al., *The QCD Equation of State to $O(\mu_B^6)$ from Lattice QCD*, *Phys. Rev. D* **95** (2017) 054504 [[1701.04325](#)].
- [19] A. Bazavov et al., *Skewness and kurtosis of net baryon-number distributions at small values of the baryon chemical potential*, *Phys. Rev. D* **96** (2017) 074510 [[1708.04897](#)].
- [20] A. Bazavov et al., *Skewness, kurtosis, and the fifth and sixth order cumulants of net baryon-number distributions from lattice QCD confront high-statistics STAR data*, *Phys. Rev. D* **101** (2020) 074502 [[2001.08530](#)].
- [21] D. Bollweg et al., *Equation of state and speed of sound of (2+1)-flavor qcd in strangeness-neutral matter at non-vanishing net baryon-number density*, [2212.09043](#).
- [22] D. Bollweg, J. Goswami, O. Kaczmarek, F. Karsch, S. Mukherjee, P. Petreczky et al., *Second order cumulants of conserved charge fluctuations revisited: Vanishing chemical potentials*, *Phys. Rev. D* **104** (2021) [[2107.10011](#)].
- [23] J. Goswami, F. Karsch, S. Mukherjee, P. Petreczky and C. Schmidt, *Conserved charge fluctuations at vanishing net-baryon density from Lattice QCD*, *EPJ Web Conf.* **259** (2022) 10010 [[2109.00268](#)].
- [24] D. A. Clarke, *Isothermal and isentropic speed of sound in (2+1)-flavor qcd at non-zero baryon chemical potential*, *PoS LATTICE2022* (2022) 147 [[2212.10009](#)].
- [25] A. Bazavov et al., *Chiral crossover in QCD at zero and non-zero chemical potentials*, *Phys. Lett. B* **795** (2019) 15 [[1812.08235](#)].